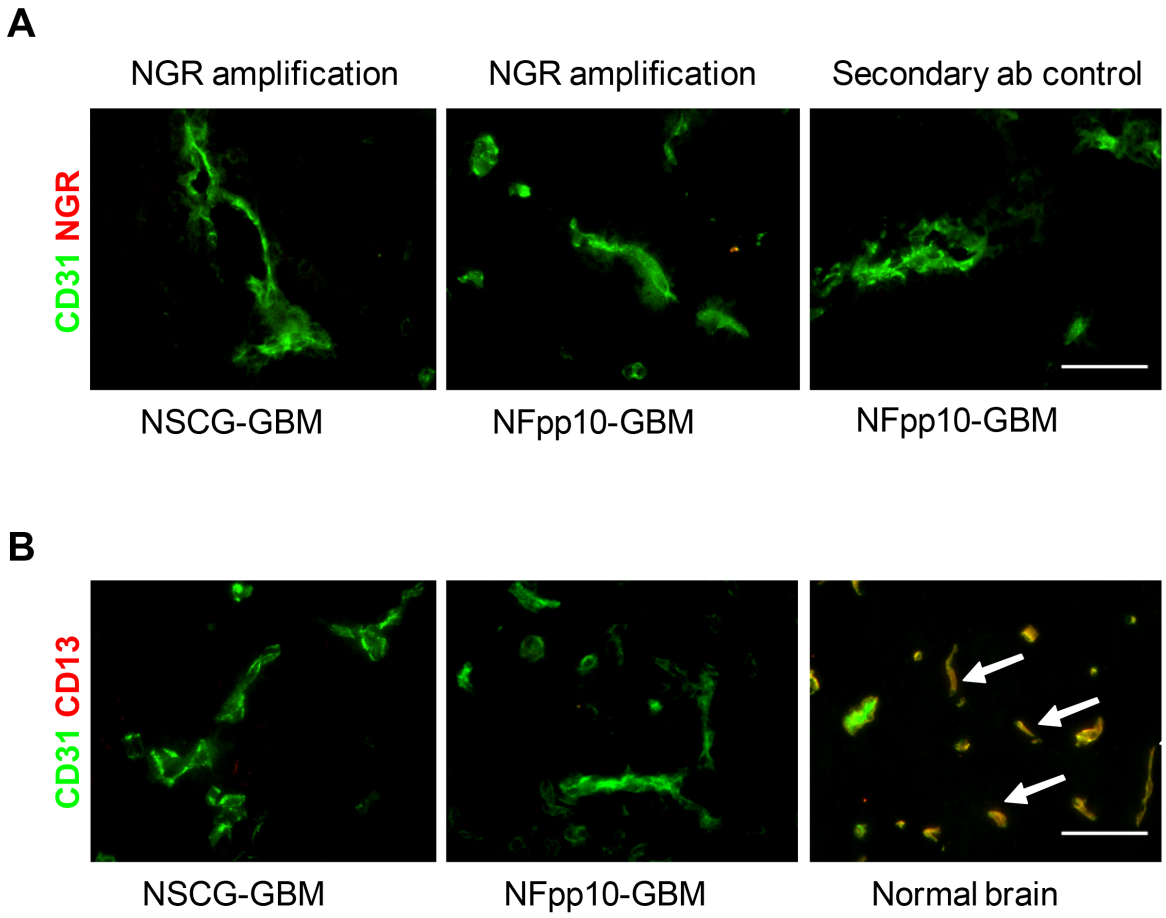

Figure S1. Murine GBM lack CD13 expression and NGR binding. (A) Immunohistochemical analysis of FAM-NGR loaded micelle homing *in vivo* (red) to $CD31^+$ tumour vessels (green) in NSCG-GBM (left) or NFpp10-GBM (middle) using a goat anti-FITC/anti-goat-Cy3 signal amplification step (NGR amplification); secondary antibody (ab) control refers to staining of NFpp10-GBM with anti-goat-Cy3 secondary antibody only, omitting the anti-FITC detection step (right). (B) Immunohistochemical analysis of CD13 expression (red) in NSCG-GBM (left) or NFpp10-GBM (middle) in relation to $CD31^+$ blood vessels (green), and CD13 coverage of blood vessels in normal brain (right) as control. Arrows depict some $CD13^+$ $CD31^+$ (yellow) blood vessels. Scale bars, 50 µm.

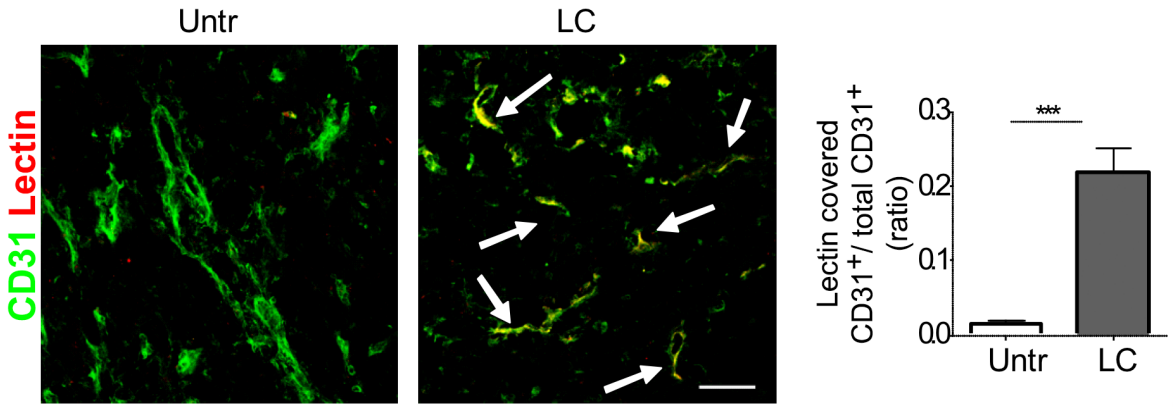

Figure S2. LIGHT-CGKRK treatment increased tumour perfusion. NFpp10-GBM bearing mice were left untreated (Untr) or treated with 20 ng LIGHT-CGKRK (LC) for 2 weeks followed by assessment of tumour perfusion after injection of fluorescently-labelled lectin. Representative histology, showing overlay of $CD31^+$ vessels (green) with fluorescent lectin (red); arrows depict blood vessels covered by overlapping markers (yellow). Quantification of perfused vessels (yellow) (n=2 mice/group, 50-100 blood vessels/mouse). ***P=0.0001, Student's t-test. Scale bar, 50 µm.

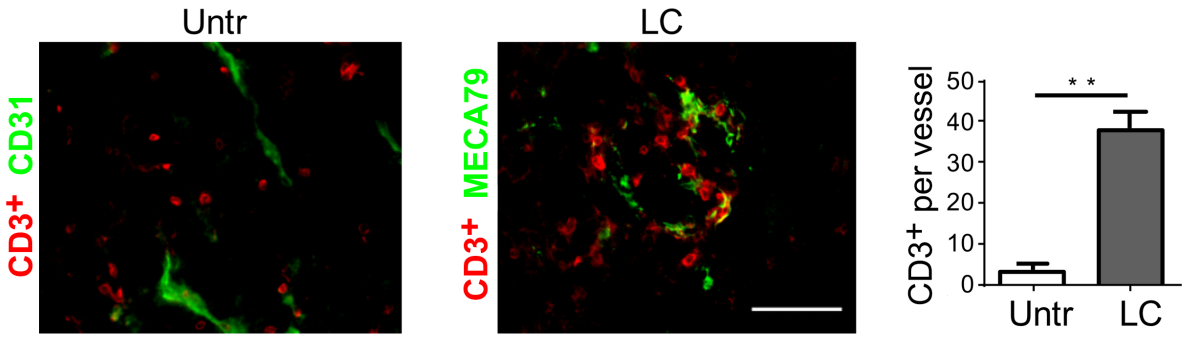

Figure S3. Intratumoural T cells clustered around HEVs but not CD31$^+$ endothelia. Immunohistochemical analysis of CD31$^+$ blood vessels (green) in untreated NFpp10-GBM in correlation to infiltrating CD3$^+$ T cells (red, left), and MECA79$^+$ HEVs (green) in LIGHT-CGKRK (LC)-treated GBM in correlation to CD3$^+$ T cells (red right). Clustering of CD3$^+$ T cells within a 50 µm radius around CD31$^+$ vessels (Untr) or HEVs (LC) was quantified, n=3, ***P*=0.0012. Student's *t*-test. Scale bar, 50 µm.

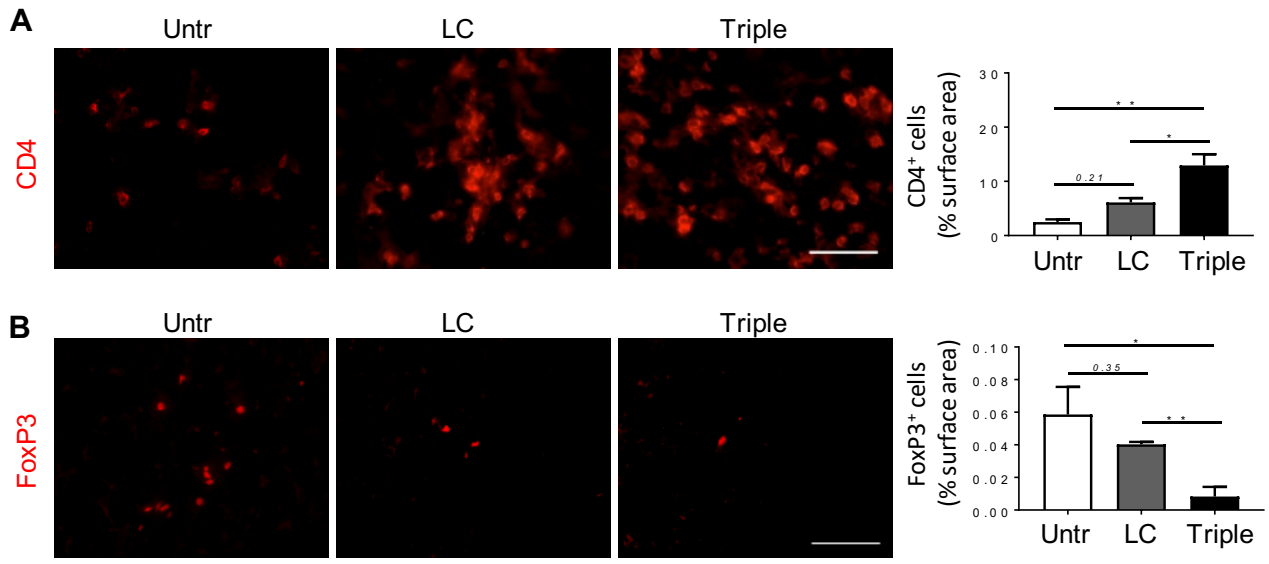

Figure S4. Increased CD4$^+$ T cell infiltration correlated with reduced intratumoral FoxP3 signals. (A) Mice bearing NFpp10-GBM were left untreated (Untr), treated for 2 weeks with LIGHT-CGKRK (LC) as single reagent, or combined with anti-VEGF/anti-PD-L1 treatment (Triple). Tumours were analysed for CD4$^+$ T cell infiltration, n=3, **P*=0.03, ***P*=0.003. (B) Quantification of FoxP3$^+$ cells in corresponding treatment groups, n=3, **P*=0.05, ***P*=0.007. ANOVA. Scale bars, 50 µm.

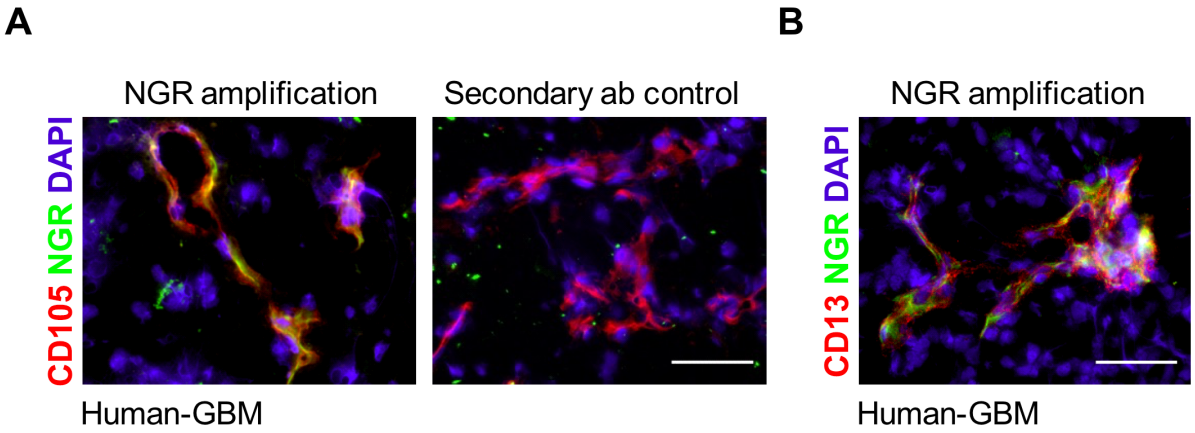

Figure S5. NGR-FAM binding to human GBM blood vessels correlated with CD13 expression. (A) Immunohistochemical analysis of FAM-NGR binding (green) to $CD105^{+}$ tumour vessels (red) in human GBM (left) using a goat anti-FITC/anti-goat-AF488 signal amplification step (NGR amplification), and control staining without anti-FITC antibody (right, secondary ab control). (B) Co-localization of amplified NGR-FAM signals (green) with CD13 (red) on human GBM tumour vessels. Scale bars, 50 µm.